JGR Biogeosciences

Key Points:

- Riparian trees in Mediterranean-type ecosystems are generally buffered against drought stress by subsurface lateral inputs
- Dry snow droughts (low P) cause greater loss of biomass in upslope and riparian trees than early snow loss during wet and warm snow droughts
- Wet and warm snow droughts can increase riparian water stress as compared to upslope sites, potentially threatening riparian microrefugia

Supporting Information:

Supporting Information may be found in the online version of this article.

Correspondence to:

L. J. Graup,
lgraup@bren.ucsb.edu

Subsurface Lateral Flows Buffer Riparian Water Stress Against Snow Drought

L. J. Graup[1] [ID]**, C. L. Tague[1], A. A. Harpold[2]** [ID]**, and S. A. Krogh[3]** [ID]

[1]University of California Santa Barbara, Santa Barbara, CA, USA, [2]University of Nevada Reno, Reno, NV, USA, [3]University of Concepción, Chillán, Chile

Abstract In the Sierra Nevada, CA, the Mediterranean climate exposes montane forests to water stress during the summer drought. Normally, spring snowmelt alleviates summer water stress, especially in riparian ecosystems that receive subsurface lateral inputs from groundwater. However, snow drought could potentially eliminate these beneficial effects. This research investigates how subsurface lateral redistribution mediates hillslope-scale vegetation responses to snow drought. We apply a spatially-distributed ecohydrologic model (Regional Hydro-Ecologic Simulation System (RHESSys)) to a snow-dominated watershed in the Sierra Nevada. We incorporate observed sap flow data along a hillslope to estimate relative differences in water stress for upslope and riparian sites, and constrain RHESSys drainage parameter uncertainty. Our model results show that subsurface lateral inputs buffer riparian water stress against snow drought. For all drought types, both upslope and riparian sites experience substantial losses of net primary productivity (NPP), and on average upslope sites are more adversely affected (upslope loss of NPP = 45% vs. riparian = 28%). Dry droughts from a lack of rain or snow induce substantial loss of biomass for upslope and riparian trees because of low annual precipitation, but a small snowpack retained during cold, dry years slightly alleviates these effects and delays water stress by 2 weeks in riparian areas and 3 weeks upslope. While riparian forests are often buffered against drought stress, our study also shows that riparian forests can suffer from water stress. We found 21% of drought scenarios where riparian trees experience greater water stress than upslope trees that were mostly associated with wet and warm snow droughts.

Plain Language Summary Climate change is increasing the frequency and severity of droughts. Combined with higher temperatures, droughts are causing widespread forest mortality. Drought-induced tree death is especially relevant to the California Sierra Nevada, which experiences wet winters and dry summers. The mountain snowpack is essential for storing winter snow that becomes spring snowmelt, which in turn fills soil water stores for trees before the summer drought. However, rising temperatures are preventing the snowpack from accumulating even in wet years, causing warm snow droughts. Here we seek to understand the consequences of changing snowpacks on forest water stress by using a computer model to explore how a tree's position on a hillslope influences its drought response. Riparian trees near the river benefit from access to lateral inputs from groundwater that provide supplemental water during seasonal drought, as compared to upslope trees that do not receive lateral inputs. Our results show that generally these lateral water inputs buffer riparian trees against drought stress though, due to loss of the snowpack, there are cases where riparian trees experience greater water stress than upslope trees. As droughts become more frequent and severe, riparian trees may be the only source of refuge in a parched landscape.

1. Introduction

Globally, forests are facing high rates of mortality from drought and heat stress (Adams et al., 2012; Allen et al., 2010). In semi-arid biomes, the patterns of tree mortality are broadly linked to different species' responses to water stress (Férriz et al., 2021; Mueller et al., 2005). Vegetation water stress is especially relevant in Mediterranean-type ecosystems (MTEs), such as the California (CA) Sierra Nevada, characterized by a seasonal summer drought following winter precipitation. In many MTEs, the mountain snowpack plays a crucial role in the water cycle by storing the winter snow that becomes spring snowmelt (López-Moreno et al., 2017), which in turn fills soil and surface reservoirs before the summer drought. Both forest vegetation and summer streamflow depend on this snow storage that is at risk of disappearing as the climate warms (Siirila-Woodburn et al., 2021). With climate change dramatically altering snowpacks, it is imperative to understand the impacts on seasonal and multi-year vegetation water stress.

The Sierra Nevada is expected to receive less precipitation in the future (Strzepek et al., 2010; Swain et al., 2018), and warmer temperatures will cause less of it to fall as snow (Cayan et al., 2008; Diffenbaugh et al., 2015), creating a "snow drought" (Rhoades et al., 2018). Dry snow droughts occur during dry years when there is low precipitation, both rain and snow. However, even during a wet year, warm snow droughts can occur when more precipitation falls as rain and there are more midwinter melt events (Harpold et al., 2017). Conversely, dry but snowy conditions can produce drought when most of the precipitation falls as snow during a cold winter (Hatchett et al., 2022). The type of drought is likely to influence the partitioning of incoming precipitation between evapotranspiration (ET) and runoff. In general, a snow-to-rain transition often shifts the partitioning of precipitation to increase ET and decrease runoff (Berghuijs et al., 2014; Hammond et al., 2019). However, in MTEs, the dominance of winter snow can lead to ET declines with a loss of spring snowmelt (Tague & Peng, 2013). For both dry and warm snow droughts, less snowfall means less snowmelt and less water available in the spring, leading to an earlier and longer summer drought (Harpold, 2016). Previous studies have shown that reduced water availability during summer increases vegetation water stress, exacerbating forest mortality and fire risk (Boisrame et al., 2019; Crockett & Westerling, 2018; Harpold, 2016). Even in small watersheds, however, there is substantial spatial heterogeneity in water availability and forest sensitivity to changes in precipitation and snowmelt (Tague et al., 2019; Young et al., 2017).

Spatial heterogeneity of forest water stress is influenced by local availability of plant-accessible water (Bales et al., 2018; McLaughlin et al., 2020) and plant water-use strategies (Grossiord et al., 2014; Hwang et al., 2009; Phillips et al., 2016). On a hillslope, topography controls snow accumulation and melt, and the lateral redistribution of subsurface water (Brooks et al., 2015; Williams et al., 2009). These processes are tightly linked in complex terrain to influence vegetation water supply and consequently, spatial and temporal patterns of forest water stress (Hoylman et al., 2018, 2019; Kampf et al., 2014; Tromp-van Meerveld & McDonnell, 2006). Hillslope-scale patterns of forest structure often reflect multi-year acclimations to these topographic controls on water availability (Bolstad et al., 2001; Mackay & Band, 1997)—for example, riparian forests support greater biomass and diversity of plant species (Fan, 2015; Gregory et al., 1991; Naiman et al., 2010). Forest structural differences along a hillslope, especially in convergent sites, could also be due to variations in soil texture (Gwak & Kim, 2016), nutrient accumulation (Mackay, 2001), or plant trait acclimation (Tai et al., 2018). These variables often covary due to interactions between hydrologic redistribution and nutrient flowpaths (McClain et al., 2003). Subsurface lateral inputs carry nitrogen and other nutrients, which can influence potential differences in soil fertility in riparian environments and resulting plant community composition (Weintraub et al., 2017). As droughts become more frequent, these hydrological microrefugia may no longer mitigate water stress (Hawthorne & Miniat, 2016; McLaughlin et al., 2017; Mueller et al., 2005; Tai et al., 2021).

In MTEs, seasonal water limitations often magnify the role of topography, snowmelt, and groundwater in generating patterns of forest water stress (Cooper et al., 2020). In the spring, the snowmelt pulse enhances groundwater recharge which augments and delays the slow release of groundwater to the riparian area (Safeeq et al., 2013). These lateral inputs allow riparian vegetation productivity to continue into the summer drought (Figure 1a). In sensitive Sierra Nevada headwater ecosystems, subsurface lateral redistribution is critical to support riparian ecosystem services, such as enhancing biodiversity (Spencer et al., 1983), improving water quality (Gergans et al., 2011), and reducing downstream flooding (Erman et al., 1988). A lush riparian corridor not only benefits animals and birds as habitat, but the dense canopy also creates the shade needed to keep the river cool for fish (Butler & Hawthorne, 1968; Erman et al., 1988). Riparian shading may become more critical as the climate warms and flow regimes change (Meyers et al., 2010). The loss of riparian habitat would jeopardize important hydrological microrefugia for many sensitive animals.

Tree ecophysiological responses to drought along a hillslope are mediated by subsurface lateral flows and water subsidies in ways that are modified by snowmelt amount and timing. It is unclear how snow droughts will influence the buffering effect of lateral inputs in riparian forests. In water-limited ecosystems, riparian areas benefit from access to additional water and nutrients from upslope areas throughout the seasonal drought, contributing to greater biomass of riparian trees than upslope trees (Fan, 2015). Greater biomass, however, increases water demand and requires more photosynthesis to maintain which can lead to greater sensitivity to climate variability (Tai et al., 2020). We hypothesize that the greater biomass of riparian trees may also make them more susceptible to water stress under extended severe drought conditions, as opposed to upslope trees which do not receive lateral inputs (Figure 1b). To our knowledge, no one has investigated the potential influence of lateral water contributions to the vulnerability of riparian forests to snow drought in MTEs. Considering nearly one third of global land
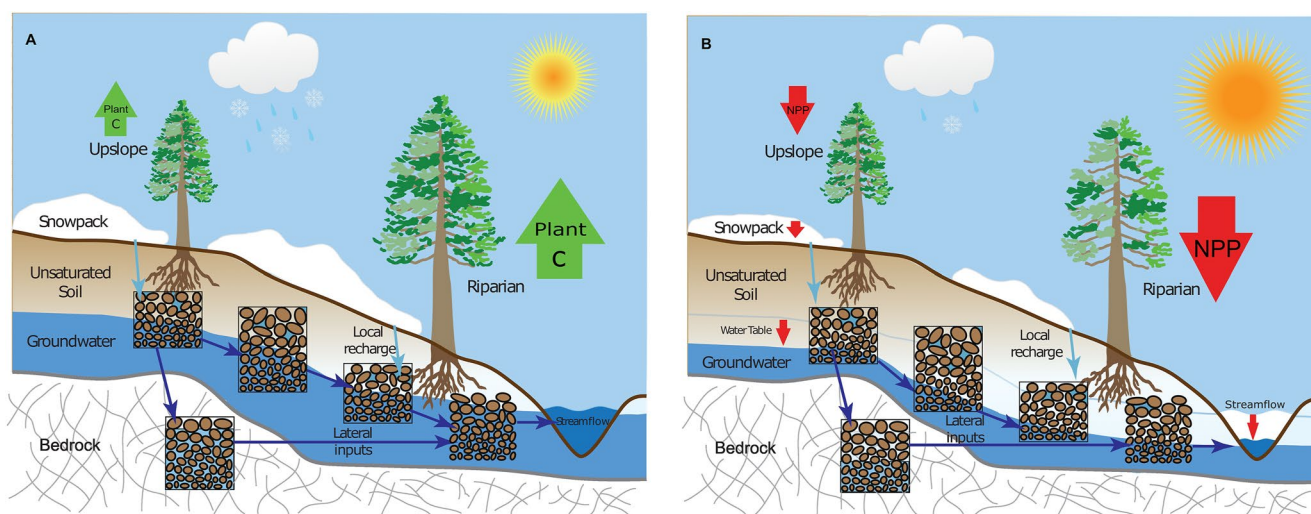
Figure 1. Conceptual model of hillslope ecohydrology demonstrating (a) long-term hillslope-scale forest structure, with expected greater accumulation of plant carbon (C) in riparian trees and (b) hypothetical riparian drought response scenario, with greater decline of net primary productivity (NPP) in riparian trees compared to upslope trees.

area has vegetation with access to shallow groundwater (Fan et al., 2013), it is important to consider how riparian buffering effects will be modified by climate change.

Although there are multiple factors that contribute to riparian forests' fertile microenvironment, their role as refugia is due primarily to enhanced water availability from lateral inputs, especially in semi-arid environments such as the Sierra Nevada (McLaughlin et al., 2017). However, examining vegetation responses to drought through observations alone is complicated by interactions between antecedent climate and snowfall, subsurface hydrology, and plant ecophysiology. In this paper, we develop a simple conceptual model of hillslope ecohydrology (Figure 1) to guide modeling experiments that investigate how changing snowpacks with a warming climate may influence vegetation water use and water stress in both upslope and riparian forests. We focus specifically on how upslope water subsidies in riparian microrefugia might lead to differential drought responses in riparian versus upland forests.

A key question is how to model and predict the length and types of droughts that will be severe enough to lead to biomass declines in riparian trees. Mechanistic models can serve as virtual laboratories to disentangle the multiple, interacting controls on forest water use and its sensitivity to drought (Fatichi et al., 2016). Answering this question, however, requires modeling the partitioning of subsurface water along a hillslope, a major uncertainty in hydrologic modeling (McDonnell et al., 2007). This uncertainty arises partially due to our inability to observe subsurface patterns of rooting structures, soil water holding capacity, and lateral redistribution over annual timescales (Cooper et al., 2020; Thompson et al., 2011). To adequately represent our conceptual model, we accept necessary tradeoffs that allow dynamic ecophysiological response, simulation of subsurface water storage and lateral redistribution, and the ability to perturb climate, while neglecting explicit 3-D detail of subsurface characteristics. Fortunately, process-based models that link hydrology and vegetation growth allow us to use observations of aboveground vegetation productivity and water use to infer subsurface drainage and storage properties (Dralle et al., 2020; Thompson et al., 2011), and more importantly here, the hydrologic connectivity between upslope and riparian sites (Hwang et al., 2012). The Regional Hydro-Ecologic Simulation System (RHESSys) is a sophisticated ecohydrologic model that has been used to simulate all of the processes relevant to our conceptual model, with adequately proven representations of dynamic vegetation growth and subsurface hydrology (Garcia et al., 2016; Hwang et al., 2012; Tague & Peng, 2013).

In this study, we use RHESSys, applied to an experimental hillslope in the Sierra Nevada, CA, to investigate how lateral inputs may alter the sensitivity of riparian versus upslope forest water use and net productivity under different types of droughts. The study site is strategically located near the altitude of the rain-snow transition, making it highly sensitive to climate warming. We take advantage of sap flow data measured in both riparian and upslope trees to constrain model parameters that influence the timing and magnitude of lateral connectivity
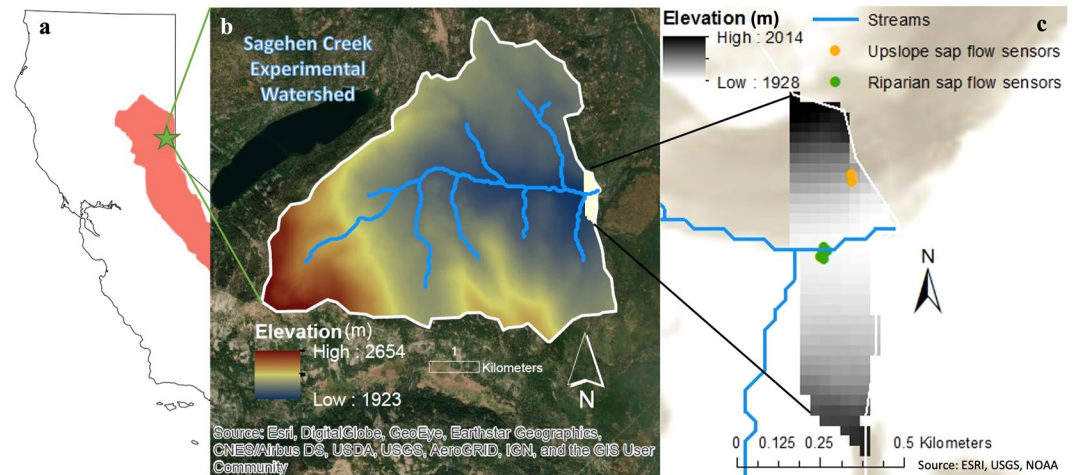
Figure 2. (a) Location of study site in the Sierra Nevada, CA; (b) Sagehen Creek Watershed delineation, highlighted area denotes experimental hillslope; (c) location of sap flow sensors along hillslope.

between upslope and riparian sites. Hypothetical drought experiments extrapolate the observed upslope-riparian differences in water stress across natural climate variability. These experiments address our research questions: (a) how does subsurface lateral redistribution influence seasonal water stress over multiple drought years? (b) How will these responses change for dry versus warm snow drought?

2. Methods

2.1. Study Site

2.1.1. Sagehen Creek Experimental Watershed

Sagehen Creek Experimental Watershed, hereafter referred to as Sagehen, is a 27 km^2 watershed located in the central Sierra Nevada, California (Figure 2). Sagehen has a Mediterranean climate with warm, dry summers and cold, wet winters. Mean annual precipitation is 880 mm. The watershed receives a mix of rain and snow, but most of it falls as snow between November and April. Vegetation is predominantly mixed conifer forest, dominated by ponderosa pine (*Pinus ponderosa*), lodgepole pine (*Pinus contorta*) and Jeffrey pine (*Pinus jeffreyi*) at lower elevations which is replaced by white fir (*Abies concolor*), red fir (*Abies magnifica*), mountain hemlock (*Tsuga mertensiana*) and white pine (*Pinus strobus*) at higher elevations. Soils are classified as Alfisols, composed of recent alluvium, colluvium and glacial till deposits, especially near the stream channel. Lithology consists of Miocene-Pliocene basaltic and andesitic lava flows, which overlie deep volcaniclastic deposits supporting a large groundwater aquifer system (Sylvester & Raines, 2017). The entire basin overlies the granodiorite of the Sierra Nevada batholith. Elevations range from 1,923 to 2,654 masl. This study focuses on an experimental hillslope with detailed observations that ranges between 1,928 and 2,014 masl. There are numerous non-forested areas composed of montane meadows along riparian areas and various spring-fed locations at higher elevations, reflecting the importance of groundwater dynamics in this watershed.

The site was selected as representative of a mid-elevation, mid-latitude site due to its availability of multiple, co-located, and long-term data sets, such as precipitation, air temperature, snow depth, and streamflow. A complete, quality-controlled, and gap-filled record of meteorological data has been made available and covers the period between 1966 and 2018 (Petersky & Harpold, 2018). This data is used to force our ecohydrological model and is described in Text S1 in Supporting Information S1. The base station is from the Western Regional Climate Center (WRCC) network station (originally a NOAA Co-op meteorological station) located near the USGS stream gauge (elevation 1,923 masl). To distribute data from the WRCC station across the hillslope, we calculate air temperature and precipitation lapse rates (details provided in Text S1 and Figure S1 in Supporting Information S1), as orographic effects are significant in the Sierra Nevada, particularly for large, synoptic storms (O'Hara et al., 2009) and cold-air pooling (Cayan et al., 2019).
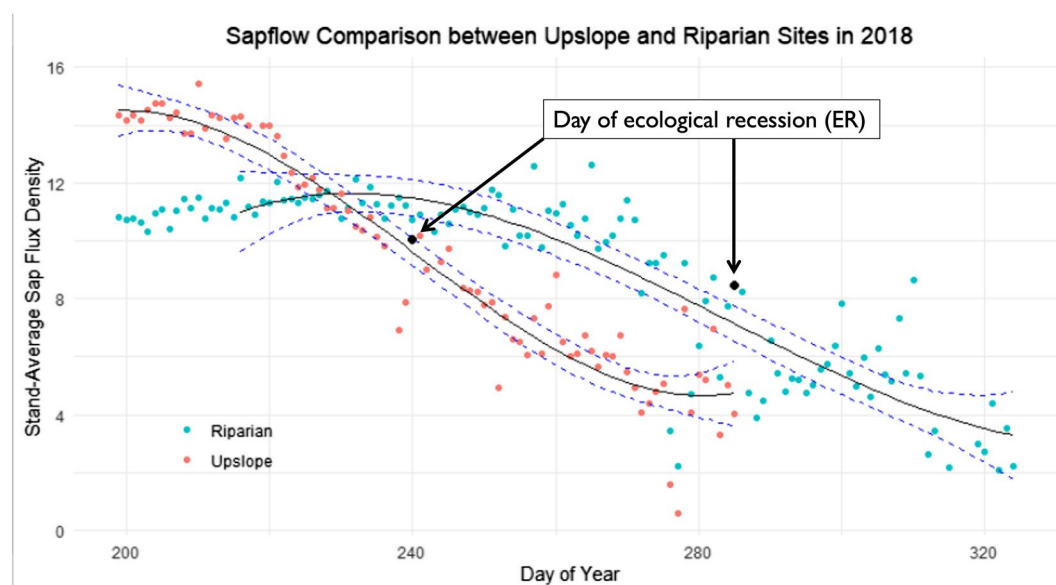
Figure 3. Graphical depiction of calibration metric, the difference in day of ecological recession between upslope and riparian stands (ER_diff), derived from peak daily sap flow data.

2.1.2. Sap Flow Analysis

An intensive observation campaign has been conducted along the experimental hillslope to obtain sap flow measurements with paired micrometeorology and flux tower measurements (Cooper et al., 2020). We use these records to evaluate differences between riparian and upslope vegetation water use. The sap flow sensors (Thermal Dissipation Probes, TDP30, Dynamax, Inc.) were placed along the experimental hillslope from the riparian area to the upper section of the hillslope (Figure 2), to represent the effect of the topographic gradient on tree's transpiration. There were two tree stands measured (riparian and upslope), with each stand including sensors on 6–10 individual trees. The riparian site contained lodgepole pines of varying sizes, while the upslope site is a mix of lodgepole and Jeffrey pines of similar size. Sap flow was measured throughout the summers of 2018–2020, with short periods removed due to technical issues. For a full description of raw sap flux data processing, refer to Cooper et al. (2020). Sap flux density was recovered at 15-min intervals and aggregated to mean daily values to remove diurnal variation and preserve the seasonal trend.

To aid model calibration, we derived a metric from the observed sap flow data. Since scaling tree sap flux density to stand transpiration adds additional uncertainty due to problems in the estimation of sapwood area (Hernandez-Santana et al., 2015), we instead capture the timing of summer water stress for an individual tree, defined here as *the day of ecological recession* (ER)—the day of the year that represents the inflection point of a cubic polynomial fitted to the declining daily sap flow data (Figure 3). The use of the cubic polynomial fitted to the sap flow curve serves a dual purpose: (a) to remove daily fluctuations caused by intermittent rain or clouds which more effectively captures the annual recession, and (b) to easily calculate the inflection point from an equation. Since the data is relatively sparse, we bootstrapped the calculation by sampling points from the full data set and derived a confidence interval for $\alpha = 0.10$. We derived ER from the stand-average sap flow at the upslope and riparian sites separately and calculated the difference (ER_diff). The ER_diff in 2018 was 45 days, in 2019 was 29 days, and in 2020 was 41 days, which highlights the benefit that riparian trees receive from lateral inputs to extend their growing season (Figure 3). We use ER_diff to examine the effect of lateral redistribution on vegetation water use. We acknowledge that differences in timing of water stress may also reflect spatial differences in climatic forcing. However, our analysis of meteorological data for this site suggests that these differences are small (Table S4 in Supporting Information S1). We also note that we are using this difference here to calibrate effective subsurface drainage parameters in the ecohydrological model which are designed to account for spatial differences in climate forcing as well as vegetation structure.

2.2. RHESSys Model

RHESSys (Tague & Band, 2004; Tague et al., 2013) is a physically-based model that incorporates spatially-distributed cycling of water, carbon and nitrogen (RHESSys v7.3). RHESSys is partitioned into spatial hierarchies with the watershed discretized into subbasins composed of two hillslopes, which are further divided into spatially explicit model grid cells grouped by topography, vegetation, and soils. The modeling grid is scaled with respect to topographic routing, usually 30 m, to allow lateral moisture redistribution along the hillslope. The spatially explicit grid cell also supports finer-scale heterogeneity of vegetation that allows for local routing of water and nutrients within a grid cell (Burke & Tague, 2019; Burke et al., 2021). Each model grid cell can be split into aspatial patches of open space (i.e., grass cover) and multiple forest stands which are assumed to be well-mixed and can potentially share water, depending on rooting parameters. The forested patch contains canopy layers that represent a stand of overstory trees and/or understory shrubs and grasses. Algorithms describing interception of rainfall by the canopy, and wind and solar radiation attenuation through the canopy account for tree height, leaf area, and canopy gap fraction. Downwelling solar and longwave radiation is adjusted by topographic aspect following MT-CLIM (Running et al., 1987). Water fluxes, including evaporation from soil, litter, intercepted rainfall, and canopy transpiration, are modeled by the Penman-Monteith equation (Monteith, 1965). Stomatal conductance is computed with the Jarvis model (Jarvis et al., 1976), which accounts for solar radiation, vapor pressure deficit (VPD), soil moisture, and air temperature. RHESSys uses daily climate forcing and plant ecophysiology parameterization to estimate daily fluxes of vegetation carbon, nitrogen, and water to simulate tree growth. Gross Primary Production is calculated with the Farquhar equation (Farquhar et al., 1980), and maintenance and growth respiration are estimated to calculate Net Primary Productivity (NPP). NPP is allocated to leaf, stem, root, and non-structural carbohydrates (NSC) storage carbon pools according to resource allocation strategies to replace leaf, branch, and fine root annual turnover (Garcia et al., 2016). Since stomatal conductance is limited by water availability, and transpiration influences plant growth, the hydrology and ecosystem carbon cycling models are coupled. Ecophysiological parameters adjust the plant hydrologic and carbon and nitrogen cycling sub-models to account for species differences (see Table S3 in Supporting Information S1). For a complete description of RHESSys algorithms, refer to Tague and Band (2004), Tague et al. (2013), and the RHESSys website (https://github.com/RHESSys/RHESSys/wiki) for details on more recent updates.

The hydrologic sub-model simulates vertical soil moisture fluxes between four stores within each patch: surface detention, rooting-zone unsaturated store, saturated zone, and a seasonal snowpack. Snowmelt is estimated using a combination of an energy budget approach for radiation-driven melt with an air temperature index-based approach for sensible and latent heat-driven melt processes and advective controls for rain on snow events. Snowmelt, throughfall and rainfall percolate into the soil from the detention store based on Phillip's infiltration equation (Phillip, 1957). Vertical drainage from the unsaturated zone to the saturated zone is limited by field capacity, and by the vertical unsaturated hydraulic conductivity. Field capacity storage, defined by porosity, pore size index, and air entry pressure, influences the amount of soil moisture available to plants within their rooting zone. Soil drainage occurs when soil water is above field capacity, allowing this excess water to be redistributed downslope in the saturated zone. Lateral redistribution of subsurface water takes place at spatial grid cell level, where infiltrated water is shared by vegetation between aspatial patches within a single grid cell and is then routed downslope towards the hillslope outlet. Model parameters determine how quickly this infiltration and soil drainage takes place—vertical and shallow subsurface lateral drainage rates depend on saturated hydraulic conductivity and its decay with depth (Table S1 in Supporting Information S1). Although RHESSys does not explicitly model subsurface pressure gradients, the subsurface routing module does account for both shallow and deeper groundwater flows. A certain proportion of infiltrated water is assumed to follow macropores and bypass the soil matrix of the rooting zone to recharge deep groundwater stores in bedrock. This deep groundwater is then routed to the riparian area through a linear-discharge relationship. In this way, riparian trees can receive lateral inputs from subsurface redistribution in the shallow, saturated zone and bypass flow from deeper groundwater. The riparian area is defined as the 30 m pixels in a Digital Elevation Model containing the stream. The natural flood plain may extend beyond this range, but the width of this zone is sufficient to capture the effect of topographic convergence on valley-bottom plant communities.

2.3. Model Calibration

In ecohydrological models, there is substantial uncertainty in subsurface storage and drainage parameters and ecophysiology parameters controlling photosynthetic efficiency, allometric relationships, carbon allocation, and

mortality. Uncertainty in storage and drainage parameters comes from heterogeneity in subsurface material, including substrate type and presence of fractures or macropores (Atchley & Maxwell, 2011; Hartmann, 2016; McDonnell et al., 2007), and uncertainty in plant rooting depth and distributions (Fan et al., 2017; Germon et al., 2020; Yang et al., 2016). Ecophysiological uncertainty is related to broad variation in plant functional type parameters (Masson et al., 2003; White et al., 2000), as well as local plant adaptations (Ackerly et al., 2000). Given these multiple sources of parameter uncertainty, model calibration is required to constrain parameter ranges by comparing model output against field observations. However, due to equifinality (Beven, 2006), complex, nonlinear environmental models can produce the same output for varying sets of input parameters. Behavioral modeling resolves this issue by incorporating only realistic model realizations (based on site observations and ecophysiological literature) and sacrificing the notion of a perfect model (since there is no such thing). Using this methodology, we capture the effect of RHESSys parameter uncertainty in a measure of statistical likelihood that incorporates the ability of the model to match observations, while accounting for parameter interaction effects (Beven & Binley, 1992).

Our model calibration routine followed a two-step process: first, we subset behavioral ecophysiological parameters that ensure the carbon cycling sub-model for an average patch provides a reasonable representation of expected forest stand conditions for this region (spatially-lumped calibration), and second, we calibrated drainage parameters at the hillslope scale (spatially-distributed calibration). For both steps, we sample uniformly across parameter distributions to run model simulations and compare RHESSys output with a suite of observations. Initial parameter distributions come from standard RHESSys parameter libraries (https://github.com/RHESSys/ParamDB) or species- and site-specific values in literature (see Tables S1 and S2 in Supporting Information S1 for complete list of initial parameter ranges). We iteratively updated initial uniform parameter distributions by comparing model output against observations, described below, until behavioral parameter distributions were found.

We use calibration against observed ER_diff for spatially-distributed calibration, and comparison against Lidar and literature ranges of plant carbon pools for spatially-lumped calibration (Table S3 in Supporting Information S1). Lidar has been flown over Sagehen numerous times, so we can not only estimate canopy height but also change in height and biomass over time (Text S2 in Supporting Information S1). For plant carbon pools, following Garcia et al. (2016), we used published data for Ponderosa pine since there is a large body of literature on measured carbon stores (Chatterjee et al., 2009; Law et al., 2001). We incorporated additional literature on Jeffrey pine (Johnson et al., 2008) and Lodgepole pine (Chatterjee et al., 2009) to broaden the observed carbon stores (Table S3 in Supporting Information S1) and preliminary ecophysiology parameter ranges (White et al., 2000; Table S2 in Supporting Information S1). Ecohydrological models such as RHESSys account for species differences through ecophysiological parameters. Different species tend to have different ranges for key parameters such as specific leaf area, stomatal conductance, and carbon allocation. Because we retain uncertainty across many degrees of freedom of ecophysiology parameters, we are able to account for cross species differences in these parameters and implicitly represent species effects. We argue that the model representation of vegetation could adequately capture growth behavior for multiple species of Sierra Nevada conifers, but we cannot identify which parameter sets relate to which species. Thus, this definition of vegetation does not attempt to simulate a single species, but rather uses multiple behavioral parameter sets as a first-order approximation of the likely range of species behaviors in a mixed-conifer forest similar to those at Sagehen.

Before running simulations, ecohydrological models require a "spin-up" period for the carbon (C) and nitrogen (N) cycling routines to achieve a steady state. First, soil C and N stores were stabilized, usually requiring 3–4k years of simulated growth. Then, each parameter set was used to spin up a mature forest by setting plant carbon stores to zero and running the model for 150 years to represent average present-day stand ages in Sagehen (Adam Csank, personal communication). Since the WRCC climate record is only 50 years old, RHESSys repeated the climate record for the full 150-year simulation.

2.3.1. Spatially-Lumped Calibration

The objective of the spatially-lumped calibration was to verify the accuracy of the carbon cycling sub-model in RHESSys. At this scale, we considered 23 ecophysiology parameters and five soil parameters that define field capacity, wilting point, and local subsurface partitioning of groundwater (refer to Table S2 in Supporting Information S1 for a complete list of ecophysiological parameters). To compare RHESSys against observations, we calculate mean stem carbon, height, and leaf area index (LAI) from the last 10 years of the 150-year spin-up to

simulate a mature forest stand. Comparison against Lidar measurements of tree height and change in height over time (Figure S2, Text S2 in Supporting Information S1) and literature estimates of carbon stores for representative mixed-conifer tree species (Table S3 in Supporting Information S1) validates the model's ability to simulate average forest stand conditions.

Figure S2 in Supporting Information S1 presents a comparison of RHESSys model output with Lidar data measured in Sagehen (described in Text S2 in Supporting Information S1). The Lidar boxplots show individual trees within a 4,500 m^2 area corresponding to the RHESSys grid cell used for spatially-lumped calibration. The RHESSys boxplots show estimates of tree height across parameter uncertainty, which allows the model to match the wide range of observed tree heights and growth trajectories. Following calibration, carbon pools also fall within the ranges found in the literature (Table S3 in Supporting Information S1), demonstrating that model estimates can capture realistic growth and allocation strategies for Sierra Nevada conifer species.

While this calibration step does greatly constrain behavioral parameter ranges and ensures reasonable plant carbon estimates, there are still many viable post-calibration parameter sets. For spatially-distributed calibration (and ultimately, for scenario analysis), sampling across these ranges was prohibitively computationally expensive. To reduce dimensionality for the spatially-distributed calibration, we implemented a Sobol sensitivity analysis of ecophysiology parameters. The Sobol sensitivity analysis determined the most sensitive parameters that contribute to the total variance of the model output for any output metric (Sobol, 1990). We apply the Sobol method to each RHESSys output metric for this calibration step. The Sobol sensitivity indices for each of these metrics (Figure S3 in Supporting Information S1) were used to identify which parameters contribute the least to output variance. For these parameters, we fix them to a single value, which helps to reduce computational processing time for hillslope simulations. The remaining parameter ranges are constrained to their behavioral ranges (Table S2 in Supporting Information S1) to maintain parameter uncertainty in subsequent analysis and are used in the next stage of model calibration.

2.3.2. Spatially-Distributed Calibration

The objective of the spatially-distributed calibration was to constrain drainage parameters so that RHESSys could match the observed difference in timing of vegetation water stress along a hillslope. To model the experimental hillslope in Sagehen, we followed a similar spin-up procedure as above, allowing vegetation across the entire hillslope to grow according to the microclimate and drainage conditions introduced by topography. The mature hillslope was then run over the calibration period (2018–2020) to force the model with observed climate during the sap flow measurement period. At this scale, we considered 13 ecophysiological parameters that were shown to be the most sensitive in our Sobol analysis and eight soil parameters, that include local rooting zone storage parameters and vertical and lateral saturated hydraulic conductivity and their decay with depth controlling subsurface lateral redistribution. The parameters retained from the spatially-lumped calibration were set to their behavioral ranges, and the drainage parameter distributions were taken from ranges characteristic of the soil type (sandy loam).

We calibrated drainage parameters against observed ER_diff. To confirm that ER_diff also captures daily transpiration trajectories, we use the Pearson correlation coefficient. In RHESSys, the corresponding sap flow sites were defined at the finest spatial grid cell that contains the actual instrumented trees for each forest stand. Since RHESSys does not model sap flow, we estimated ER from forest stand transpiration and calculated the difference between upslope and riparian stands (ER_diff). Then, we computed a fuzzy metric of acceptability (Seibert & McDonnell, 2002), defined by a symmetric trapezoidal function that assigns a value of 1 if the modeled ER_diff is within the bootstrapped confidence interval of the sap flow-derived ER_diff and declines to 0 by one standard deviation away from the mean. Upslope-riparian ER_diff in 2018 was 45 days (Figure 3), with a bootstrapped confidence interval of about 2 weeks. We retained acceptable parameter sets (for which our fuzzy metric >0) to determine behavioral parameter ranges that represent the uncertainty in soil storage and drainage characteristics along the hillslope (Figure S4 in Supporting Information S1). The median Pearson's R for behavioral parameter sets was 0.9 for both upslope and riparian sites in 2018, and only slightly declined to 0.85 for riparian sites and 0.75 for upslope sites during 2019–2020. Subsurface parameter uncertainty is tightly constrained by this calibration strategy (Table S1 in Supporting Information S1). This calibration step was essential to verify that all of our behavioral parameter sets provide reasonable estimates of tree growth given observations, and in particular, account for upslope-riparian differences in the timing of water stress.

Table 1
Drought Type Classification

SWE \ P	> Mean (677 mm)	< Mean
> Mean (128 mm)	HPHS	LPHS
< Mean	HPLS	LPLS

Note. P and SWE are accumulated annual precipitation and snow water equivalent, respectively, on April 1st. H is high, L is low, S is SWE—HPHS is high P, high SWE; LPLS is low P, low SWE (i.e., dry snow drought); HPLS is high P, low SWE (i.e., warm snow drought), etc.

2.4. Drought Scenarios

The long-term climate record at Sagehen was used to characterize years according to their drought type. Based on the definition of snow drought (Harpold et al., 2017), we normalized April 1st snow water equivalent (SWE), which is typically used to represent peak SWE accumulation, and accumulated annual precipitation (P) by the long-term average (mean peak SWE = 128 mm, mean P = 677 mm) and applied simple classifications to discriminate between drought types (Table 1). Table 1 outlines the abbreviations that will be used to describe drought types: HPHS for big, wet years; HPLS for warm snow droughts; LPHS for dry, but snowy years; and LPLS for dry snow droughts (following Hatchett et al.'s (2022) intuitive phase diagrams of snow drought). We apply these classifications to the three SNOTEL stations which highlights elevational effects (Figure S5 in Supporting Information S1).

To single out the effects of drought type, we stitched together individual years corresponding to each classification separately to create hypothetical multi-year (4 years) model experiments. The longest consecutive drought in the historic record at Sagehen was 4 years, so we chose that length for our experiments. Using RHESSys output of hillslope-scale P and SWE, we applied the drought classifications (Figure S6 in Supporting Information S1) and selected eight median water years for each drought type (eight LPHS years defined the maximum sample size). From each sub-sample of 8 years, we randomly sampled four water years to generate random climate scenarios and repeated this process 50 times to test for climate sensitivity.

Following model calibration, we obtained 245 behavioral parameter sets. To obtain estimates of ecophysiological response variables (Table 2) for each drought type, first, each parameter set was used to spin-up the Sagehen hillslope for 150 years to simulate a mature forest. Then, every drought scenario was preceded by a control year of moderate precipitation (925 mm) to approximate antecedent wetness conditions. The total number of scenarios is the # of parameter sets (245) * # of climate sequences (50) * # of drought types (4) = 49,000 individual drought scenarios. Thus, each drought type uses 12,250 model realizations to calculate results for upslope and riparian sites. For each drought scenario, we calculated absolute change in ER and percent deviation from the control year of total ET, total NPP, maximum LAI, and minimum NSC (as a proxy for drought vulnerability) (Tague et al., 2013) at each site to capture differences in inter-annual vegetation responses (Table 2). The two-sample Kolmogorov-Smirnov test was used to evaluate significant differences across parameterization uncertainty between sites and between drought types.

Table 2
Output Metrics to Compare Upslope and Riparian Responses to Drought

Ecophysiological Variable	Units
Day of ecological recession (ER)	Day of calendar year
Annual evapotranspiration (ET)	m H_2O/year
Annual net primary productivity (NPP)	kg C/Year
Annual maximum leaf area index (LAI)	m^2/m^2
Annual minimum non-structural carbohydrates (NSC)	kg C

Table 3
Output Metrics by Drought Type Presented as "Mean (Standard Deviation)" for Upslope (U) and Riparian (R) Sites

	Comparison of deviation from control year							
	HPHS		LPHS		HPLS		LPLS	
P	17% (19%)		−45% (7%)		−13% (8%)		−59% (6%)	
SWE	39% (47%)		11% (37%)		−59% (30%)		−69% (20%)	
	U	R	U	R	U	R	U	R
NPP	57% (46%)	40% (49%)	−58% (16%)	−37% (18%)	0% (30%)	−4% (23%)	−75% (18%)	−45% (18%)
ET	19% (10%)	7% (10%)	−19% (11%)	4% (10%)	5% (7%)	6% (8%)	−42% (12%)	−4% (15%)
ER[a]	4 (30)	0 (7)	−28 (20)	−7 (13)	−3 (28)	0 (6)	−49 (26)	−20 (23)
LAI	15% (14%)	11% (10%)	1% (7%)	3% (5%)	7% (8%)	6% (6%)	1% (7%)[b]	3% (6%)
NSC	6% (6%)	3% (5%)	−1% (5%)	−1% (3%)[b]	5% (5%)	2% (4%)[b]	−4% (6%)	−1% (3%)[b]

Note. Percent deviation calculated as (drought-control)/control.

[a]ER is an absolute difference, units are in days. [b]indicates statistical insignificance at $\alpha = 0.05$.

3. Results

3.1. Upslope-Riparian Differences in Water Stress

Table 3 summarizes relative model estimates of ecophysiological output for all climate scenarios. Compared to the control year and averaged over all drought scenarios, the mean reduction in P and SWE was 39% and 53%, respectively. The historic long-term riparian advantage is clear: riparian trees support more biomass than upslope trees in the control year after the 150-year spin-up (Figure S7 in Supporting Information S1). Our results indicate that riparian trees are also buffered against drought stress. On average, riparian trees lost 28% of annual NPP, compared to a reduction of 45% for upslope trees. Although upslope-riparian differences are highly variable due to interannual climate variability, this initial greater riparian drought resilience is maintained throughout the multi-year drought, as riparian trees are able to retain more leaf area than upslope trees (Figure 4). The ability to support high LAI allows riparian sites to maintain transpiration at pre-drought levels; in fact, annual riparian transpiration remained about the same throughout the multi-year drought, even increasing by up to 25% in warm years due to an extended growing season (Figure 5). Riparian drought resilience is further demonstrated by the insignificant changes in NSC for all drought types (Table 3).

Upslope forests show larger variability in ecophysiological responses. This is evident in greater fluctuations of NPP at the upslope site compared to the riparian site across drought types (Figure 6). Since upslope trees are generally water-limited, they respond to increased water input during non-drought years with increased
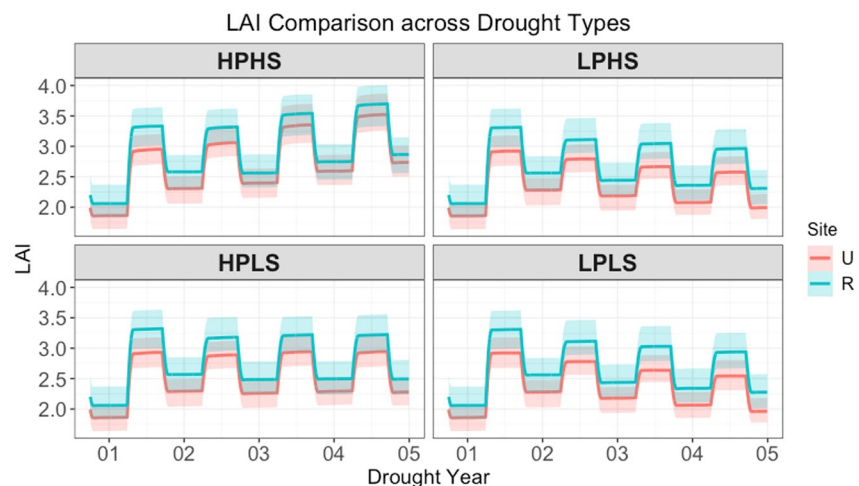

Figure 4. Comparison of LAI across drought types and years for upslope (U) and riparian (R) sites.
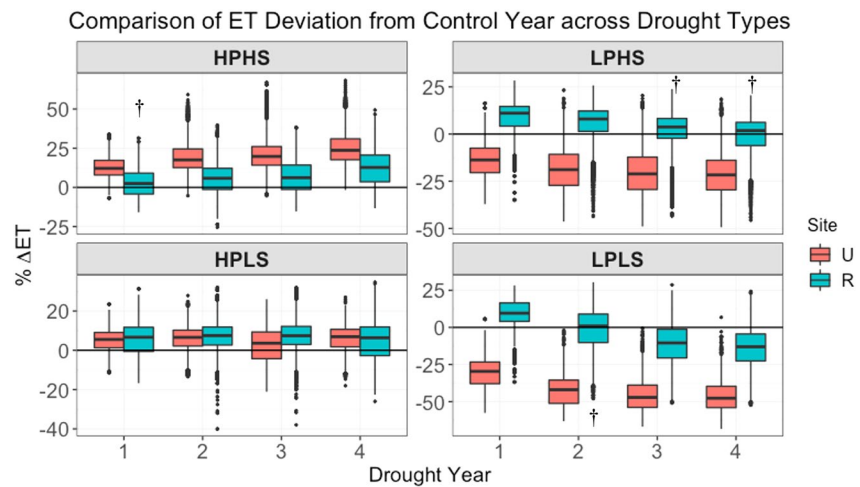
Figure 5. Comparison of ET % deviation from control year across drought types and years for upslope (U) and riparian (R) sites. † indicates insignificant difference from control year, all other results are statistically significant at $\alpha = 0.05$.

productivity and ET (Figures 5 and 6). Conversely, with decreased water input during drought, upslope trees experienced compounding effects of water stress and showed greater declines in NPP and ET (Table 3). The loss of NPP during drought scenarios translated to a drop in LAI when NPP is insufficient to compensate for annual leaf turnover (Figure 4). Upslope trees were only able to produce new leaf growth by utilizing NSC stores, which were reduced by up to 20% in the worst scenarios (Figure S8 in Supporting Information S1). Declines in LAI contributed to substantial reductions in total transpiration (up to 50%, Figure 5). Even with lower LAI, the decreased water availability with drought leads to 2 months earlier onset of water stress in upslope relative to riparian sites, as indicated by ER in Table 3.

Although on average riparian trees experience less water stress than upslope trees, there were parameter set-climate combinations that show greater stress in riparian trees. Out of all modeled drought years, we find that 21% of scenarios yield at least a 5% (for significance) greater reduction (or smaller increase) in riparian NPP compared to upslope NPP. That number increases to 32% when we include the HPHS scenarios. We note that these scenarios may reflect either particular parameter sets or drought sequences (recall that each drought scenario includes 50 random climate sequences). Further analysis found that for all parameter sets, there were hypothetical drought sequences that resulted in greater riparian water stress. To isolate the effect of parameter uncertainty alone, we average over all climate sequences to derive four consecutive drought years for each parameter set and drought
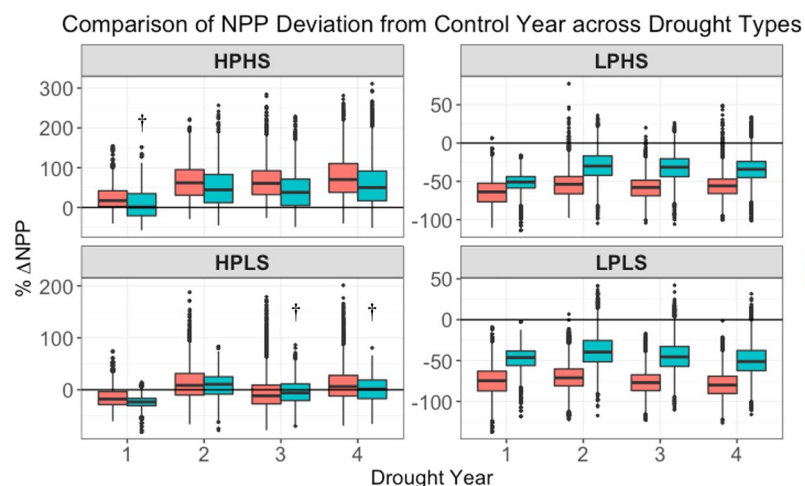

Figure 6. Comparison of NPP % deviation from control year across drought types and years for upslope (U) and riparian (R) sites. † indicates insignificant difference from control year, all other results are statistically significant at $\alpha = 0.05$.

type. Out of 245 parameter sets, 186 exhibit greater riparian water stress in any given year of the 4 year drought when results are averaged over all climate sequences, compared to 243 that yield greater upslope water stress in any given year. These distributions need not be mutually exclusive since a year in which riparian trees experience less water stress than upslope could be followed by a year in which riparian water stress is greater, depending on climate variability. However, that leaves two parameter sets for which the average water stress is greater in riparian trees for every single year. These parameter sets are distinguished by differences in subsurface storage and drainage: slower decay in hydraulic conductivity with depth ($p = 0.03$), lower available water storage capacity ($p < 0.001$), and higher wilting point ($p < 0.001$). Slower decay in hydraulic conductivity increases drainage rates for high subsurface flows when the hillslope would be hydrologically connected, which moves more water out of the riparian zone. Combined with lower available water storage, lateral inputs will not provide as much extra water to supplement riparian productivity (Figure 1b). A higher wilting point causes trees to stop transpiring sooner during the summer drought. These factors all interact to reduce the buffering effect of lateral inputs to riparian trees, increasing water stress.

We also compare the 18 parameter sets in Figure S7 in Supporting Information S1 that yield upslope plant C > riparian plant C after spin-up to the 227 parameter sets that match our expectations of greater riparian plant C (Figure 1a). The significant differences between these parameter distributions are related to stomatal conductance, rooting depth and subsurface drainage. Parameter sets that yield larger upslope trees tend to have lower maximum stomatal conductance ($p = 0.007$), deeper roots ($p = 0.03$), and higher hydraulic conductivity ($p = 0.004$) than parameter sets for which riparian trees support more carbon. Lower stomatal conductance improves water use efficiency to the benefit of upslope trees. Deeper roots provide upslope trees greater access to water, supplementing local recharge but not lateral inputs for riparian trees. Higher hydraulic conductivity moves water through the subsurface quicker, transferring water out of the riparian zone before the trees can use it. This forces riparian trees to rely more on local recharge, which causes riparian forest structure to resemble upslope forests over the long-term (Figure 1a).

3.2. Hillslope-Scale Effects Vary by Drought Type and Duration

To explore how hillslope responses change due to drought type and throughout the drought period, we break out each output metric (Table 2) across drought type and over time. While years sampled within each drought type conform to the broad drought classification, there is variability in magnitude and timing of precipitation and temperature forcing. Over 4 years, the average reduction in P from the control year was 59% for LPLS, 45% for LPHS, and 13% for HPLS (Table 3). Similarly, SWE was reduced by 69% for LPLS, 59% for HPLS, and increased by 11% for LPHS. Randomized interannual variability is small for most cases, compared to the effect of drought type.

The change in NPP relative to the control year is highly variable across all drought scenarios. Upslope trees generally experience a greater reduction in NPP than riparian trees across all 3 drought types, but the effect is more severe for years with low P than for high P, low SWE (HPLS). LPLS (and LPHS) years exhibit a 75% and 45% (58% and 37%) reduction in upslope and riparian NPP respectively, while HPLS years show little difference. Riparian NPP had a slight decrease, but the mean change in upslope NPP was not significantly different from zero (Table 3). HPLS years also demonstrate potential for large positive increases in NPP relative to the control year in 42% of years, for both upslope and riparian sites, compared to ∼1% for low P years (Figure 6). Over 50% of these more productive HPLS cases are upslope trees, with an average increase in NPP of 28% relative to the control year compared to 20% for riparian trees. This suggests that upslope trees benefit from the warmer temperatures when there is sufficient water availability, and are less affected by loss of the snowpack than riparian trees.

In RHESSys, declines in NPP translate into declines in new growth and overall biomass as leaf turnover losses cannot be replaced. We observed this effect of compounding drought stress in LAI throughout the four consecutive years (Figure 4). For all drought types, there was no significant change in LAI in the first drought year, showing that biomass changes are generally a lagged response to drought stress. However, as the drought continues, reductions in LAI became progressively worse. Low P years exhibited large reductions in LAI by the fourth year, with both upslope and riparian sites losing up to 15% of LAI. Since riparian trees have greater LAI, this translates to a greater absolute loss of riparian canopy cover (-0.45 m²/m² vs. -0.38 m²/m² upslope). HPLS years, on the other hand, saw moderate increases in LAI that were maintained throughout the multi-year drought period.

As trees lose leaf area, they must support photosynthetic and respiratory demands with stored NSC. As with LAI, we observed compounding drought stress in NSC (Figure S8 in Supporting Information S1). By the fourth year of low P, upslope trees used about 10% of NSC on average but up to 35%, while riparian trees only used about 3% of NSC on average but up to 25% in the worst cases. Since HPLS years did not cause reductions in LAI, there were increases in NSC at both sites, but upslope NSC increased by twice as much as riparian NSC on average and changes in riparian NSC were not significant.

As a result of these structural changes in tree physiology, transpiration exhibited some interesting behavior (Figure 5). For low P years, ET shows a declining trend where later years during the drought show larger reductions than earlier years, likely due to decreasing LAI with multiple years of drought stress. For all drought types, riparian ET actually increases, by about 6%–10% on average, in the first few years. However, by the third year of LPLS, riparian ET declines by 11% on average relative to the control year, due to multi-year declines in deeper groundwater stores. LPHS scenarios are able to maintain riparian ET on average, but upslope sites are very stressed (-20% ET by the second year). HPLS years show consistent increases in ET relative to the control year for both upslope (5%) and riparian (6%) sites. Variable transpiration behavior is also evident in comparing absolute changes in ER from the control year (Figure S9 in Supporting Information S1). Riparian ER stayed relatively stable throughout all years, except later years of LPLS; whereas upslope ER is much more sensitive. The low P scenarios shift upslope ER earlier by a month to 6 weeks, while HPLS years showed little change on average in ER, but with a large range of up to a month difference.

Parameter uncertainty accounts for most of the variability in vegetation responses to drought for a particular drought type, compared to climate uncertainty. For those scenarios that exhibit greater riparian water stress, we find a relationship between drought type and upslope-riparian NPP. Out of the 21% of drought scenarios for which the reduction in riparian NPP is greater than that of upslope, 86% of those cases occur during HPLS years, with 12% during LPHS years and only 2% during LPLS years. The percent difference between upslope and riparian sites is also significantly greater during HPLS years ($p < 0.001$): median upslope NPP was on average 86% greater than riparian NPP compared to 15% and 18% for LPLS and LPHS years, respectively (Figure S10 in Supporting Information S1). The percent difference in NPP between LPLS and LPHS was not significant for the subset of scenarios considered here, although in general the effect of these drought types on the percent difference between upslope and riparian sites is significantly different ($p < 0.001$).

4. Discussion

This research uses RHESSys to compare relative differences in vegetation responses between upslope and riparian forest stands and their sensitivity to various multi-year drought scenarios. Our observed and modeled data show the beneficial role that lateral inputs provide to riparian vegetation communities to buffer them against drought stress. The degree of water stress is altered by drought type for both upslope and riparian forests. There is a clear distinction between large reductions in productivity with low P droughts (LPHS, LPLS), and weaker stress responses with warm snow droughts (HPLS). While in general riparian sites are buffered against drought stress, we found that riparian water stress can be greater than upslope stress during certain warm snow drought (HPLS) scenarios, potentially threatening riparian microrefugia.

4.1. Methodological Considerations

Our study does include several simplifying assumptions that are important to acknowledge. We represent an idealized hillslope that conforms to our conceptual model in order to eliminate confounding factors from other ecological variables or hydrological processes. This simplification in model setup allows us to focus on the effect of lateral inputs from groundwater on upslope-riparian differences in tree water stress. Our conceptual model assumes that hillslope variation in soil characteristics, such as soil depth and porosity, or species' differences in rooting depth and climate sensitivity are small relative to the effect of lateral redistribution. Similarly, we are ignoring the structural variation in species composition and nutrient availability along a wetness gradient from dry upslope areas to wet riparian areas. We recognize that species differences, natural succession processes, changes in nutrient cycling and spatially heterogeneous soil texture may also play a role in upslope-riparian responses to drought. Some of this variation is captured in our behavioral parameter uncertainty, but more field observations are needed to explore all of these variables concomitantly and consider species' effects explicitly.

We acknowledge that our model validation is restricted to comparison with stand-scale estimates of sap flow and tree height, but aggregating this data was necessary since we are focused on plot-scale averages rather than individual tree responses. Future studies might expand on this by collecting data from multiple hillslopes and incorporating additional observations such as flux tower data. The inferences derived from our results are interpreted within the limited context presented in this study, and are not meant to be predictions of future responses to climate change. Specific drought responses will likely vary depending on subsurface conditions, groundwater systems, tree species or climate regimes.

On our small hillslope (86 m relief), spatial variation in microclimate effects along a topographic gradient are minor. The mean difference in peak SWE between upslope and riparian sites in RHESSys is 15 mm (which is 12% of total upslope SWE), while mean upslope VPD is only 1% greater than riparian VPD (Table S4 in Supporting Information S1). However, for larger hillslopes and watersheds, upslope and riparian distinctions in drought responses are likely to also be influenced by differences in microclimate.

Our definition of drought types is a step in recognizing the variable nature of hydrological drought in mountainous terrain. The methods used here to represent droughts are, however, a simplification of "real" climate and should be interpreted as end-members of a multi-year drought in a snow-dominated climate. Although 4 years of drought has been observed in the historic record, that length was chosen to represent the extreme case and still capture the effects of a shorter drought. We use multiple drought sequences to account for climate uncertainty, but do not vary the control year used before each climate scenario. It is possible that much wetter or drier antecedent moisture conditions could affect drought responses.

In summary, while our model application does not attempt to describe the experimental hillslope exactly, it captures the general observed behavior that allows us to consider the contribution of lateral flows to riparian and upslope ecohydrological responses for different drought types. The Sagehen hillslope is an example of a broad range of mid-elevation conifer-dominated watersheds within the central Sierra Nevada. The methods presented here can be applied to investigate how geologically-diverse watersheds with different groundwater systems, or higher precipitation within the Sierra Nevada will respond to snow drought.

4.2. Influence of Lateral Redistribution on Vegetation Water Stress

Vulnerability to drought induces plant responses in RHESSys that are consistent with ecophysiological expectations of water stress (Fatichi et al., 2016). Since RHESSys models stomatal conductance as a function of soil water potential, transpiration begins to decline as soon as plant-available water becomes limited. The day of ER characterizes this behavior to show how upslope trees experience water stress much earlier than riparian trees. For most scenarios, riparian ER remained stable throughout the drought, indicating that riparian trees were not water-limited; whereas upslope trees saw large reductions in transpiration and earlier onset of water stress (Figure 5, Figure S9 in Supporting Information S1). Since upslope trees must rely on local recharge to supply transpiration, they are at greater risk of water stress during dry years than riparian trees. The widening difference in ER as the drought progresses (Figure S9 in Supporting Information S1) suggests greater vulnerability at upslope sites than riparian sites, in contrast to our hypothesis (Figure 1b). Sustained water limitation leads to downregulation of photosynthesis, which is evident in decreased NPP in the first year (Figure 6). By the second year, the loss of NPP limits new growth and forces the trees to use NSC to replace turnover losses and support maintenance respiration (Figure S8 in Supporting Information S1). At this point, trees are highly vulnerable to drought stress since they are running a photosynthetic deficit. Prolonged deficits lead to leaf area declines as trees can no longer maintain as much biomass. Upslope trees use more NSC and lose more LAI, increasing their vulnerability to mortality (McDowell et al., 2011). Riparian trees are able to delay these responses compared to upslope trees, even while sustaining more leaf area (riparian LAI = 2.8 vs. 2.5 upslope, $p < 0.001$), due to their access to lateral inputs from groundwater.

Our findings show that the resilience of riparian plant communities reflects the buffering effect of subsurface lateral flows throughout multi-year droughts. Recent research using isotopes has shown that remotely recharged water (i.e., lateral inputs) supplies up to 47% of transpiration in riparian forests (Miguez-Macho & Fan, 2021), and as much as 100% during the dry season in MTEs (Barbeta & Peñuelas, 2017). In this study, lateral inputs provided riparian trees with 66% greater ET on average relative to upslope trees (Figure 5), an extra 7 weeks of

productivity during the dry season (Figure S9 in Supporting Information S1), and 17% greater NPP (Figure 6). We also show how drought interacts with subsurface lateral flows to preserve riparian areas as a refuge that support higher ET and biomass, even as the rest of the watershed may experience substantial water stress. If we exclude the wettest years (HPHS), and only consider drought effects, then riparian trees benefit from 83% greater ET, 2 months later ER, and 37% greater NPP than upslope trees. Without riparian forest access to shallow groundwater, these hydrological microrefugia, and the species that depend on them, would not exist (McLaughlin et al., 2017).

Our model experiments demonstrate that for the majority of scenarios (79%), riparian NPP declines but remains greater than upslope sites throughout the drought. These results align with field-based studies in semi-arid regions that found drought responses of riparian vegetation were dependent on water table levels (Garssen et al., 2014; Hinojosa-Huerta et al., 2013; Scott et al., 1999). Similarly, tree mortality in riparian stands was less severe than in upslope stands in an MTE in Spain (Lloret et al., 2004) and semi-arid region in Colorado (Tai et al., 2017). These patterns of mortality are controlled by shallow groundwater levels driven by topographically-induced lateral flow that override climate effects (Fan et al., 2013). Although we do not explicitly model forest mortality, greater reliance on NSC in upslope trees (−10% vs. −3% in riparian trees by 4th year of dry snow drought, Figure S8 in Supporting Information S1) suggests declines in within-tree resources that can be used for defense against insects and maintenance of healthy plant function as a proxy for vulnerability to mortality (Tague et al., 2013). Our results support the need for global climate models to account for topographic effects on lateral redistribution to accurately capture the patterns of soil moisture and drought water stress under climate change (Fan et al., 2019; Kim & Mohanty, 2015; Kollet & Maxwell, 2008).

Observed variation in tree responses to drought stress are driven by between- and within-species differences in plant water use and carbon allocation, as well as fine-scale heterogeneity in soil properties (McDowell et al., 2008). We capture this variability in our behavioral ranges of ecophysiology and drainage parameter uncertainty, constrained by field observations, to demonstrate sensitivity of real-world responses to plant trait and environmental characteristics. Estimates of the long-term forest structure with model spin-up generally show greater riparian plant carbon (Figure S7 in Supporting Information S1). The subset of parameter sets that contradicted this response showed significant differences in rooting depth, maximum stomatal conductance, and subsurface hydraulic conductivity—two of these parameters, rooting depth and subsurface hydraulic conductivity, are notoriously difficult to measure and may vary substantially at plot, hillslope and landscape scales. Our model estimates also suggest that even when riparian trees had more carbon, greater riparian water stress can occur, as noted above, due to interactions between climate variability and soil water availability. The decay of subsurface hydraulic conductivity, wilting point, and available water storage capacity all contribute to reduce the buffering effect of lateral inputs on riparian drought response.

4.3. Snow-Climate Variability Influences Hillslope Ecohydrological Interactions

Interannual climate variation exposes Sagehen Creek Watershed and similar watersheds in the California Sierra Nevada to a wide range of drought types, frequency, and severity. Although the natural range of precipitation variability includes warm and dry snow droughts, dry snow droughts are becoming more prevalent in this area due to climate change (Hatchett & McEvoy, 2018). Historically, dry snow droughts (LPLS), usually accompanied by warmer temperatures, have induced the most severe tree mortality events (Allen et al., 2015; Anderegg et al., 2013). Our results suggest that increasing temperatures that shift precipitation from snow to rain cause moderate impacts on forest productivity, but the most severe forest water stress impacts, including loss of NPP, NSC, and total biomass, arise from an overall lack of precipitation during dry snow droughts (LPLS). Our research is consistent with other studies that argue that climate warming will continue to push forests toward productivity declines and ultimately mortality thresholds (Allen et al., 2010; Van Mantgem & Stephenson, 2007).

On a hillslope, the snowpack is essential to store winter precipitation to supply summer transpiration, and produce a large pulse of spring snowmelt to generate lateral flow and groundwater recharge. The snowpack retained during dry, but snowy years (LPHS) helps to alleviate some water stress, as evidenced by the increase in ET at both upslope (39%) and riparian (8%) sites, compared to dry snow droughts (LPLS) (Table 3). During a warm snow drought (HPLS), the wet winters fill soil water stores to supply ET, but without the snowpack to delay the timing of water input, more of the growing season is water-limited. The large variability in warm snow

drought (HPLS) NPP responses compared to low P droughts is due to variation in the timing of winter water input (Table 3, Figure 5). Warmer temperatures, particularly during the early growing season, can also increase productivity and transpiration (Table 3, Figure 5), which has been observed in the Sierra Nevada and the Swiss Alps (Bales et al., 2018; Mastrotheodoros et al., 2020), although these effects are elevation-dependent (Gilbert & Maxwell, 2018). While there is uncertainty about how precipitation will change in the Sierra Nevada, almost all climate models predict declines in snow because of warmer temperatures (Cayan et al., 2008).

Although riparian trees were generally buffered against drought stress, there were multiple instances (21%) in which riparian NPP decreased more than upslope NPP. Note that these scenarios reflect particular ecophysiology and drainage parameter sets in combination with particular climate sequences. The majority of these cases occurred during warm snow droughts (HPLS), which points to greater riparian sensitivity to the loss of the snowpack than upslope trees. Earlier melting of the snowpack leads to a longer growing season, which can simultaneously increase productivity earlier in the year while increasing water stress later in the year (Harpold, 2016). This explains why riparian trees may suffer disproportionately from warm snow droughts (HPLS) (Figure S10 in Supporting Information S1). Riparian trees can have "too much of a good thing" until some threshold is reached that pushes them into unstable territory. Without snowmelt providing extra water later in the season, the hillslope becomes hydrologically disconnected much sooner, to the detriment of riparian trees that can enter into a deficit if they use their available water too quickly (Lowry & Loheide., 2010; Tague & Moritz, 2019). High rates of plant water use, caused by high tree density or plant conductance, and high rates of subsurface flow combined with low soil water storage capacity that exhaust hydrologic connectivity sooner will exacerbate effects of riparian water stress.

5. Conclusion

Our model results show that across a variety of multi-year drought types, subsurface lateral inputs from groundwater may buffer riparian trees relative to upslope trees. The magnitude of this effect is modified by drought type. Dry snow droughts induce substantial loss of biomass for both upslope and riparian trees as a result of low annual precipitation, but the snowpack retained during dry, but snowy years slightly alleviates these effects and delays water stress by 2 weeks in riparian areas and 3 weeks upslope. While riparian forests are often buffered against drought stress, our study shows that in some circumstances riparian forests can suffer from water stress. In our results, there are 21% of drought scenarios where riparian trees experience greater water stress than upslope trees. Scenarios that found higher vulnerability in riparian forests were mostly associated with warm snow droughts. Riparian water stress occurs due to "too much of a good thing" where seasonal lateral inputs stimulate growth that is then dependent on this additional water. In warm snow droughts, early snowmelt combined with high spring atmospheric water demand makes the greater biomass of riparian trees more vulnerable to water stress later in the summer. While our model results do not account for all the factors that can lead to upslope/riparian differences, they demonstrate the important role played by lateral inputs and how they can contribute to counter-intuitive patterns of high riparian drought stress.

Forest density reduction has the potential to alleviate water stress. Future work could build on our results to explore if hillslope-scale treatments can reduce water stress and mitigate fire risk in upslope areas. Our research emphasizes that while riparian trees are often buffered from drought stress, they are not invulnerable. Particular combinations of tree ecophysiology parameters that vary within and between species, soil storage and drainage properties and drought sequences can lead to substantial water stress in riparian forests. While further research is needed into how specific species respond, our research suggests that riparian drought responses are an important concern. The disproportionate benefits that riparian forests provide and their potential to serve as hydrological microrefugia throughout multi-year droughts elevate their need for attention from forest managers. A focus on riparian fuel reduction management practices is relatively novel and site-specific (Broadmeadow & Nisbet, 2004; Stone et al., 2010). More research is needed to assess if and when riparian fuel reduction management practices are warranted. As droughts become more frequent and severe, riparian trees may be the only source of refuge in a parched landscape.

Data Availability Statement

The RHESSys model output data used for this research analysis are provided in a HydroShare repository (Graup, 2021), named "RHESSys model output for Sagehen Creek hillslope": https://www.hydroshare.org/resource/5dfb547718ae4125b122ea890f60047b/. RHESSys v7.3 model source code is publicly available on Github, and archived on Zenodo: https://doi.org/10.5281/zenodo.7191399.

References

Ackerly, D. D., Dudley, S. A., Sultan, S. E., Schmitt, J., Coleman, J. S., Linder, C. R., et al. (2000). The evolution of plant ecophysiological traits: Recent advances and future directions: New research addresses natural selection, genetic constraints, and the adaptive evolution of plant ecophysiological traits. *BioScience*, *50*(11), 979–995. https://doi.org/10.1641/0006-3568(2000)050[0979:TEOPET]2.0.CO;2

Adams, H. D., Luce, C. H., Breshears, D. D., Allen, C. D., Weiler, M., Hale, V. C., et al. (2012). Ecohydrological consequences of drought- and infestation- triggered tree die-off: Insights and hypotheses. *Ecohydrology*, *5*(2), 145–159. https://doi.org/10.1002/eco.233

Allen, C. D., Breshears, D. D., & McDowell, N. G. (2015). On underestimation of global vulnerability to tree mortality and forest die-off from hotter drought in the Anthropocene. *Ecosphere*, *6*(8), art129. https://doi.org/10.1890/ES15-00203.1

Allen, C. D., Macalady, A. K., Chenchouni, H., Bachelet, D., McDowell, N., Vennetier, M., et al. (2010). A global overview of drought and heat-induced tree mortality reveals emerging climate change risks for forests. *Forest Ecology and Management*, *259*(4), 660–684. https://doi.org/10.1016/j.foreco.2009.09.001

Anderegg, W. R. L., Kane, J. M., & Anderegg, L. D. L. (2013). Consequences of widespread tree mortality triggered by drought and temperature stress. *Nature Climate Change*, *3*(1), 30–36. https://doi.org/10.1038/nclimate1635

Atchley, A. L., & Maxwell, R. M. (2011). Influences of subsurface heterogeneity and vegetation cover on soil moisture, surface temperature and evapotranspiration at hillslope scales. *Hydrogeology Journal*, *19*(2), 289–305. https://doi.org/10.1007/s10040-010-0690-1

Bales, R. C., Goulden, M. L., Hunsaker, C. T., Conklin, M. H., Hartsough, P. C., O'Geen, A. T., et al. (2018). Mechanisms controlling the impact of multi-year drought on mountain hydrology. *Scientific Reports*, *8*(1), 690. https://doi.org/10.1038/s41598-017-19007-0

Barbeta, A., & Peñuelas, J. (2017). Relative contribution of groundwater to plant transpiration estimated with stable isotopes. *Scientific Reports*, *7*(1), 10580. https://doi.org/10.1038/s41598-017-09643-x

Berghuijs, W. R., Woods, R. A., & Hrachowitz, M. (2014). A precipitation shift from snow towards rain leads to a decrease in streamflow. *Nature Climate Change*, *4*(7), 583–586. https://doi.org/10.1038/nclimate2246

Beven, K. (2006). A manifesto for the equifinality thesis. *Journal of Hydrology*, *320*(1), 18–36. https://doi.org/10.1016/j.jhydrol.2005.07.007

Beven, K., & Binley, A. (1992). The future of distributed models: Model calibration and uncertainty prediction. *Hydrological Processes*, *6*(3), 279–298. https://doi.org/10.1002/hyp.3360060305

Boisramé, G. F. S., Thompson, S. E., Tague, C., & Stephens, S. L. (2019). Restoring a natural fire regime alters the water balance of a Sierra Nevada catchment. *Water Resources Research*, *55*(7), 5751–5769. https://doi.org/10.1029/2018WR024098

Bolstad, P., Vose, J., & McNulty, S. (2001). Forest Productivity, leaf area, and terrain in southern Appalachian deciduous forests. *Forest Science*, *47*(3), 419–427. https://doi.org/10.1093/forestscience/47.3.419

Broadmeadow, S., & Nisbet, T. R. (2004). The effects of riparian forest management on the freshwater environment: A literature review of best management practice. *Hydrology and Earth System Sciences*, *8*(3), 286–305. https://doi.org/10.5194/hess-8-286-2004

Brooks, P. D., Chorover, J., Fan, Y., Godsey, S. E., Maxwell, R. M., McNamara, J. P., & Tague, C. (2015). Hydrological partitioning in the critical zone: Recent advances and opportunities for developing transferable understanding of water cycle dynamics. *Water Resources Research*, *51*(9), 6973–6987. https://doi.org/10.1002/2015WR017039

Burke, W., & Tague, N. (2019). *Multiscale routing—Integrating the tree-scale effects of disturbance into a watershed ecohydrologic model* (p. H53O-2022). AGU.

Burke, W. D., Tague, C., Kennedy, M. C., & Moritz, M. A. (2021). Understanding how fuel treatments interact with climate and biophysical setting to affect fire, water, and forest health: A process-based modeling approach. *Frontiers in Forests and Global Change*, *3*, 143. https://doi.org/10.3389/ffgc.2020.591162

Butler, R. L., & Hawthorne, V. M. (1968). The reactions of dominant trout to changes in overhead artificial cover. *Transactions of the American Fisheries Society*, *97*(1), 37–41. https://doi.org/10.1577/1548-8659(1968)97[37:TRODTT]2.0.CO;2

Cayan, D. R., Goodrich, J. P., Buhler, M., & Dulen, D. (2019). Cold air pooling during summer heat waves in California's Sierra Nevada (p. GC44B-03).

Cayan, D. R., Maurer, E. P., Dettinger, M. D., Tyree, M., & Hayhoe, K. (2008). Climate change scenarios for the California region. *Climatic Change*, *87*(1), 21–42. https://doi.org/10.1007/s10584-007-9377-6

Chatterjee, A., Vance, G. F., & Tinker, D. B. (2009). Carbon pools of managed and unmanaged stands of ponderosa and lodgepole pine forests in Wyoming. *Canadian Journal of Forest Research*, *39*(10), 1893–1900. https://doi.org/10.1139/X09-112

Cooper, A. E., Kirchner, J. W., Wolf, S., Lombardozzi, D. L., Sullivan, B. W., Tyler, S. W., & Harpold, A. A. (2020). Snowmelt causes different limitations on transpiration in a Sierra Nevada conifer forest. *Agricultural and Forest Meteorology*, *291*, 108089. https://doi.org/10.1016/j.agrformet.2020.108089

Crockett, J. L., & Westerling, A. L. (2018). Greater temperature and precipitation extremes intensify Western U.S. droughts, wildfire severity, and Sierra Nevada tree mortality. *Journal of Climate*, *31*(1), 341–354. https://doi.org/10.1175/JCLI-D-17-0254.1

Diffenbaugh, N. S., Swain, D. L., & Touma, D. (2015). Anthropogenic warming has increased drought risk in California. *Proceedings of the National Academy of Sciences*, *112*(13), 3931–3936. https://doi.org/10.1073/pnas.1422385112

Dralle, D. N., Hahm, W. J., Rempe, D. M., Karst, N., Anderegg, L. D. L., Thompson, S. E., et al. (2020). Plants as sensors: Vegetation response to rainfall predicts root-zone water storage capacity in Mediterranean-type climates. *Environmental Research Letters*, *15*(10), 104074. https://doi.org/10.1088/1748-9326/abb10b

Erman, D. C., Andrews, E. D., & Yoder-Williams, M. (1988). Effects of winter floods on fishes in the Sierra Nevada. *Canadian Journal of Fisheries and Aquatic Sciences*, *45*(12), 2195–2200. https://doi.org/10.1139/f88-255

Fan, Y. (2015). Groundwater in the Earth's critical zone: Relevance to large-scale patterns and processes. *Water Resources Research*, *51*(5), 3052–3069. https://doi.org/10.1002/2015WR017037

Fan, Y., Clark, M., Lawrence, D. M., Swenson, S., Band, L. E., Brantley, S. L., et al. (2019). Hillslope hydrology in global change research and Earth system modeling. *Water Resources Research*, *55*(2), 1737–1772. https://doi.org/10.1029/2018WR023903

Fan, Y., Li, H., & Miguez-Macho, G. (2013). Global patterns of groundwater table depth. *Science*, *339*(6122), 940–943. https://doi.org/10.1126/science.1229881

Fan, Y., Miguez-Macho, G., Jobbágy, E. G., Jackson, R. B., & Otero-Casal, C. (2017). Hydrologic regulation of plant rooting depth. *Proceedings of the National Academy of Sciences*, *114*(40), 10572–10577. https://doi.org/10.1073/pnas.1712381114

Farquhar, G. D., von Caemmerer, S., & Berry, J. A. (1980). A biochemical model of photosynthetic CO_2 assimilation in leaves of C3 species. *Planta*, *149*(1), 78–90. https://doi.org/10.1007/BF00386231

Fatichi, S., Vivoni, E. R., Ogden, F. L., Ivanov, V. Y., Mirus, B., Gochis, D., et al. (2016). An overview of current applications, challenges, and future trends in distributed process-based models in hydrology. *Journal of Hydrology*, *537*, 45–60. https://doi.org/10.1016/j.jhydrol.2016.03.026

Férriz, M., Martin-Benito, D., Cañellas, I., & Gea-Izquierdo, G. (2021). Sensitivity to water stress drives differential decline and mortality dynamics of three co-occurring conifers with different drought tolerance. *Forest Ecology and Management*, *486*, 118964. https://doi.org/10.1016/j.foreco.2021.118964

Garcia, E. S., Tague, C. L., & Choate, J. S. (2016). Uncertainty in carbon allocation strategy and ecophysiological parameterization influences on carbon and streamflow estimates for two Western US forested watersheds. *Ecological Modelling*, *342*, 19–33. https://doi.org/10.1016/j.ecolmodel.2016.09.021

Garssen, A. G., Verhoeven, J. T. A., & Soons, M. B. (2014). Effects of climate-induced increases in summer drought on riparian plant species: A meta-analysis. *Freshwater Biology*, *59*(5), 1052–1063. https://doi.org/10.1111/fwb.12328

Gergans, N., Miller, W. W., Johnson, D. W., Sedinger, J. S., Walker, R. F., & Blank, R. R. (2011). Runoff water quality from a Sierran upland forest, transition ecotone, and riparian wet meadow. *Soil Science Society of America Journal*, *75*(5), 1946–1957. https://doi.org/10.2136/sssaj2011.0001

Germon, A., Laclau, J.-P., Robin, A., & Jourdan, C. (2020). Tamm review: Deep fine roots in forest ecosystems: Why dig deeper? *Forest Ecology and Management*, *466*, 118135. https://doi.org/10.1016/j.foreco.2020.118135

Gilbert, J. M., & Maxwell, R. M. (2018). Contrasting warming and drought in snowmelt-dominated agricultural basins: Revealing the role of elevation gradients in regional response to temperature change. *Environmental Research Letters*, *13*(7), 074023. https://doi.org/10.1088/1748-9326/aacb38

Graup, L. (2021). RHESSys model output for Sagehen Creek hillslope, HydroShare. Retrieved from http://www.hydroshare.org/resource/5dfb547718ae4125b122ea890f60047b

Gregory, S. V., Swanson, F. J., McKee, W. A., & Cummins, K. W. (1991). An ecosystem perspective of riparian zones. *BioScience*, *41*(8), 540–551. https://doi.org/10.2307/1311607

Grossiord, C., Gessler, A., Granier, A., Pollastrini, M., Bussotti, F., & Bonal, D. (2014). Interspecific competition influences the response of oak transpiration to increasing drought stress in a mixed Mediterranean forest. *Forest Ecology and Management*, *318*, 54–61. https://doi.org/10.1016/j.foreco.2014.01.004

Gwak, Y., & Kim, S. (2016). Factors affecting soil moisture spatial variability for a humid forest hillslope. *Hydrological Processes*, *31*(2), 431–445. https://doi.org/10.1002/hyp.11039

Hammond, J. C., Harpold, A. A., Weiss, S., & Kampf, S. K. (2019). Partitioning snowmelt and rainfall in the critical zone: Effects of climate type and soil properties. *Hydrology and Earth System Sciences*, *23*(9), 3553–3570. https://doi.org/10.5194/hess-23-3553-2019

Harpold, A., Dettinger, M., & Rajagopal, S. (2017). Defining snow drought and why it matters. *Eos*, *98*. https://doi.org/10.1029/2017EO068775

Harpold, A. A. (2016). Diverging sensitivity of soil water stress to changing snowmelt timing in the Western U.S. *Advances in Water Resources*, *92*, 116–129. https://doi.org/10.1016/j.advwatres.2016.03.017

Hartmann, A. (2016). Putting the cat in the box: Why our models should consider subsurface heterogeneity at all scales. *WIREs Water*, *3*(4), 478–486. https://doi.org/10.1002/wat2.1146

Hatchett, B. J., & McEvoy, D. J. (2018). Exploring the origins of snow drought in the Northern Sierra Nevada, California. *Earth Interactions*, *22*(2), 1–13. https://doi.org/10.1175/EI-D-17-0027.1

Hatchett, B. J., Rhoades, A. M., & McEvoy, D. J. (2022). Monitoring the daily evolution and extent of snow drought. *Natural Hazards and Earth System Sciences*, *22*(3), 869–890. https://doi.org/10.5194/nhess-22-869-2022

Hawthorne, S., & Miniat, C. F. (2016). Topography may mitigate drought effects on vegetation along a hillslope gradient. *Ecohydrology*, *11*(1), e1825. https://doi.org/10.1002/eco.1825

Hernandez-Santana, V., Hernandez-Hernandez, A., Vadeboncoeur, M. A., & Asbjornsen, H. (2015). Scaling from single-point sap velocity measurements to stand transpiration in a multispecies deciduous forest: Uncertainty sources, stand structure effect, and future scenarios. *Canadian Journal of Forest Research*, *45*(11), 1489–1497. https://doi.org/10.1139/cjfr-2015-0009

Hinojosa-Huerta, O., Nagler, P. L., Carrillo-Guerrero, Y. K., & Glenn, E. P. (2013). Effects of drought on birds and riparian vegetation in the Colorado River Delta, Mexico. *Ecological Engineering*, *51*, 275–281. https://doi.org/10.1016/j.ecoleng.2012.12.082

Hoylman, Z. H., Jencso, K. G., Hu, J., Holden, Z. A., Allred, B., Dobrowski, S., et al. (2019). The topographic signature of ecosystem climate sensitivity in the Western United States. *Geophysical Research Letters*, *46*(24), 14508–14520. https://doi.org/10.1029/2019GL085546

Hoylman, Z. H., Jencso, K. G., Hu, J., Martin, J. T., Holden, Z. A., Seielstad, C. A., & Rowell, E. M. (2018). Hillslope topography mediates spatial patterns of ecosystem sensitivity to climate. *Journal of Geophysical Research: Biogeosciences*, *123*(2), 353–371. https://doi.org/10.1002/2017JG004108

Hwang, T., Band, L., & Hales, T. C. (2009). Ecosystem processes at the watershed scale: Extending optimality theory from plot to catchment. *Water Resources Research*, *45*(11), W11425. https://doi.org/10.1029/2009WR007775

Hwang, T., Band, L. E., Vose, J. M., & Tague, C. (2012). Ecosystem processes at the watershed scale: Hydrologic vegetation gradient as an indicator for lateral hydrologic connectivity of headwater catchments. *Water Resources Research*, *48*(6). https://doi.org/10.1029/2011WR011301

Jarvis, P. G., Monteith, J. L., & Weatherley, P. E. (1976). The interpretation of the variations in leaf water potential and stomatal conductance found in canopies in the field. *Philosophical Transactions of the Royal Society of London B Biological Sciences*, *273*(927), 593–610. https://doi.org/10.1098/rstb.1976.0035

Johnson, D. W., Murphy, J. D., Walker, R. F., Miller, W. W., Glass, D. W., & Todd, D. E. (2008). The combined effects of thinning and prescribed fire on carbon and nutrient budgets in a Jeffrey pine forest. *Annals of Forest Science*, *65*(6), 601. https://doi.org/10.1051/forest:2008041

Kampf, S., Markus, J., Heath, J., & Moore, C. (2014). Snowmelt runoff and soil moisture dynamics on steep subalpine hillslopes. *Hydrological Processes*, *29*(5), 712–723. https://doi.org/10.1002/hyp.10179

Kim, J., & Mohanty, B. P. (2015). Influence of lateral subsurface flow and connectivity on soil water storage in land surface modeling. *Journal of Geophysical Research: Atmospheres*, *121*(2), 704–721. https://doi.org/10.1002/2015JD024067

Kollet, S. J., & Maxwell, R. M. (2008). Capturing the influence of groundwater dynamics on land surface processes using an integrated, distributed watershed model. *Water Resources Research*, *44*(2). https://doi.org/10.1029/2007WR006004

Law, B. E., Thornton, P. E., Irvine, J., Anthoni, P. M., & Van Tuyl, S. (2001). Carbon storage and fluxes in ponderosa pine forests at different developmental stages. *Global Change Biology*, *7*(7), 755–777. https://doi.org/10.1046/j.1354-1013.2001.00439.x

Lloret, F., Siscart, D., & Dalmases, C. (2004). Canopy recovery after drought dieback in holm-oak Mediterranean forests of Catalonia (NE Spain). *Global Change Biology*, *10*(12), 2092–2099. https://doi.org/10.1111/j.1365-2486.2004.00870.x

López-Moreno, J. I., Gascoin, S., Herrero, J., Sproles, E. A., Pons, M., Alonso-González, E., et al. (2017). Different sensitivities of snowpacks to warming in Mediterranean climate mountain areas. *Environmental Research Letters*, *12*(7), 074006. https://doi.org/10.1088/1748-9326/aa70cb

Lowry, C. S., & Loheide, S. P. (2010). Groundwater-dependent vegetation: Quantifying the groundwater subsidy. *Water Resources Research*, *46*(6). https://doi.org/10.1029/2009WR008874

Mackay, D. S. (2001). Evaluation of hydrologic equilibrium in a mountainous watershed: Incorporating forest canopy spatial adjustment to soil biogeochemical processes. *Advances in Water Resources*, *24*(9–10), 1211–1227. https://doi.org/10.1016/S0309-1708(01)00040-9

Mackay, D. S., & Band, L. E. (1997). Forest ecosystem processes at the watershed scale: Dynamic coupling of distributed hydrology and canopy growth. *Hydrological Processes*, *11*(9), 1197–1217. https://doi.org/10.1002/(SICI)1099-1085(199707)11:9<1197::AID-HYP552>3.0.CO;2-W

Masson, V., Champeaux, J.-L., Chauvin, F., Meriguet, C., & Lacaze, R. (2003). A global database of land surface parameters at 1-km resolution in meteorological and climate models. *Journal of Climate*, *16*(9), 1261–1282. https://doi.org/10.1175/1520-0442(2003)16<1261:AGDOLS>2.0.CO;2

Mastrotheodoros, T., Pappas, C., Molnar, P., Burlando, P., Manoli, G., Parajka, J., et al. (2020). More green and less blue water in the Alps during warmer summers. *Nature Climate Change*, *10*(2), 155–161. https://doi.org/10.1038/s41558-019-0676-5

McClain, M. E., Boyer, E. W., Dent, C. L., Gergel, S. E., Grimm, N. B., Groffman, P. M., et al. (2003). Biogeochemical hot spots and hot moments at the interface of terrestrial and aquatic ecosystems. *Ecosystems*, *6*(4), 301–312. https://doi.org/10.1007/s10021-003-0161-9. http://www.jstor.org/stable/3659030

McDonnell, J. J., Sivapalan, M., Vaché, K., Dunn, S., Grant, G., Haggerty, R., et al. (2007). Moving beyond heterogeneity and process complexity: A new vision for watershed hydrology. *Water Resources Research*, *43*(7). https://doi.org/10.1029/2006WR005467

McDowell, N., Pockman, W. T., Allen, C. D., Breshears, D. D., Cobb, N., Kolb, T., et al. (2008). Mechanisms of plant survival and mortality during drought: Why do some plants survive while others succumb to drought? *New Phytologist*, *178*(4), 719–739. https://doi.org/10.1111/j.1469-8137.2008.02436.x

McDowell, N. G., Beerling, D. J., Breshears, D. D., Fisher, R. A., Raffa, K. F., & Stitt, M. (2011). The interdependence of mechanisms underlying climate-driven vegetation mortality. *Trends in Ecology & Evolution*, *26*(10), 523–532. https://doi.org/10.1016/j.tree.2011.06.003

McLaughlin, B. C., Ackerly, D. D., Klos, P. Z., Natali, J., Dawson, T. E., & Thompson, S. E. (2017). Hydrologic refugia, plants, and climate change. *Global Change Biology*, *23*(8), 2941–2961. https://doi.org/10.1111/gcb.13629

McLaughlin, B. C., Blakey, R., Weitz, A. P., Feng, X., Brown, B. J., Ackerly, D. D., et al. (2020). Weather underground: Subsurface hydrologic processes mediate tree vulnerability to extreme climatic drought. *Global Change Biology*, *26*(5), 3091–3107. https://doi.org/10.1111/gcb.15026

Meyers, E. M., Dobrowski, B., & Tague, C. L. (2010). Climate change impacts on flood frequency, intensity, and timing may affect trout species in Sagehen Creek, California. *Transactions of the American Fisheries Society*, *139*(6), 1657–1664. https://doi.org/10.1577/T09-192.1

Miguez-Macho, G., & Fan, Y. (2021). Spatiotemporal origin of soil water taken up by vegetation. *Nature*, *598*(7882), 624–628. https://doi.org/10.1038/s41586-021-03958-6

Monteith, J. L. (1965). Evaporation and environment. In *Symposia of the society for experimental biology* (Vol. *19*, pp. 205–234).

Mueller, R. C., Scudder, C. M., Porter, M. E., Trotter, R. T., Gehring, C. A., & Whitham, T. G. (2005). Differential tree mortality in response to severe drought: Evidence for long-term vegetation shifts. *Journal of Ecology*, *93*(6), 1085–1093. https://doi.org/10.1111/j.1365-2745.2005.01042.x

Naiman, R. J., Decamps, H., & McClain, M. E. (2010). *Riparia: Ecology, conservation, and management of streamside communities*. Elsevier.

O'Hara, B. F., Kaplan, M. L., & Underwood, S. J. (2009). Synoptic climatological analyses of extreme snowfalls in the Sierra Nevada. *Weather and Forecasting*, *24*(6), 1610–1624. https://doi.org/10.1175/2009WAF2222249.1

Petersky, R. S., & Harpold, A. A. (2018). A long-term micrometeorological and hydrological dataset across an elevation gradient in Sagehen Creek, Sierra Nevada, California [Dataset]. Zenodo. https://doi.org/10.5281/zenodo.2590799

Phillip, J. R. (1957). The theory of infiltration: 4. Sorptivity and algebraic infiltration equations. *Soil Science*, *84*(3), 257–264. https://doi.org/10.1097/00010694-195709000-00010

Phillips, R. P., Ibáñez, I., D'Orangeville, L., Hanson, P. J., Ryan, M. G., & McDowell, N. G. (2016). A belowground perspective on the drought sensitivity of forests: Towards improved understanding and simulation. *Forest Ecology and Management*, *380*, 309–320. https://doi.org/10.1016/j.foreco.2016.08.043

Rhoades, A. M., Jones, A. D., & Ullrich, P. A. (2018). The changing character of the California Sierra Nevada as a natural reservoir. *Geophysical Research Letters*, *45*(23), 13008–13019. https://doi.org/10.1029/2018GL080308

Running, S. W., Nemani, R. R., & Hungerford, R. D. (1987). Extrapolation of synoptic meteorological data in mountainous terrain and its use for simulating forest evapotranspiration and photosynthesis. *Canadian Journal of Forest Research*, *17*(6), 472–483. https://doi.org/10.1139/x87-081

Safeeq, M., Grant, G. E., Lewis, S. L., & Tague, C. L. (2013). Coupling snowpack and groundwater dynamics to interpret historical streamflow trends in the Western United States. *Hydrological Processes*, *27*(5), 655–668. https://doi.org/10.1002/hyp.9628

Scott, M. L., Shafroth, P. B., & Auble, G. T. (1999). Responses of riparian cottonwoods to alluvial water table declines. *Environmental Management*, *23*(3), 347–358. https://doi.org/10.1007/s002679900191

Seibert, J., & McDonnell, J. J. (2002). On the dialog between experimentalist and modeler in catchment hydrology: Use of soft data for multicriteria model calibration. *Water Resources Research*, *38*(11), 23-1–23-14. https://doi.org/10.1029/2001WR000978

Siirila-Woodburn, E. R., Rhoades, A. M., Hatchett, B. J., Huning, L. S., Szinai, J., Tague, C., et al. (2021). A low-to-no snow future and its impacts on water resources in the Western United States. *Nature Reviews Earth & Environment*, *2*(11), 800–819. https://doi.org/10.1038/s43017-021-00219-y

Sobol, I. M. (1990). On sensitivity estimation for nonlinear mathematical models. *Matematicheskoye Modelirovaniye*, *2*(1), 112–118.

Spencer, W. D., Barrett, R. H., & Zielinski, W. J. (1983). Marten habitat preferences in the Northern Sierra Nevada. *Journal of Wildlife Management*, *47*(4), 1181–1186. https://doi.org/10.2307/3808189

Stone, K. R., Pilliod, D. S., Dwire, K. A., Rhoades, C. C., Wollrab, S. P., & Young, M. K. (2010). Fuel reduction management practices in riparian areas of the Western USA. *Environmental Management*, *46*(1), 91–100. https://doi.org/10.1007/s00267-010-9501-7

Strzepek, K., Yohe, G., Neumann, J., & Boehlert, B. (2010). Characterizing changes in drought risk for the United States from climate change. *Environmental Research Letters*, *5*(4), 044012. https://doi.org/10.1088/1748-9326/5/4/044012

Swain, D. L., Langenbrunner, B., Neelin, J. D., & Hall, A. (2018). Increasing precipitation volatility in twenty-first-century California. *Nature Climate Change*, *8*(5), 427–433. https://doi.org/10.1038/s41558-018-0140-y

Sylvester, A., & Raines, G. (2017). *Geology of the independence lake and hobart mills 7.5' quadrangles, Nevada and Sierra counties*. California Geological Survey.

Tague, C., & Peng, H. (2013). The sensitivity of forest water use to the timing of precipitation and snowmelt recharge in the California Sierra: Implications for a warming climate. *Journal of Geophysical Research: Biogeosciences*, *118*(2), 875–887. https://doi.org/10.1002/jgrg.20073

Tague, C. L., & Band, L. E. (2004). RHESSys: Regional hydro-ecologic simulation system—An object-oriented approach to spatially distributed modeling of carbon, water, and nutrient cycling. *Earth Interactions*, *8*(19), 1–42. https://doi.org/10.1175/1087-3562(2004)8<1:RRHSSO>2.0.CO;2

Tague, C. L., McDowell, N. G., & Allen, C. D. (2013). An integrated model of environmental effects on growth, carbohydrate balance, and mortality of *Pinus ponderosa* Forests in the southern Rocky Mountains. *PLoS One*, *8*(11), e80286. https://doi.org/10.1371/journal.pone.0080286

Tague, C. L., Moritz, M., & Hanan, E. (2019). The changing water cycle: The eco-hydrologic impacts of forest density reduction in Mediterranean (seasonally dry) regions. *WIREs Water*, *6*(4), e1350. https://doi.org/10.1002/wat2.1350

Tague, C. L., & Moritz, M. A. (2019). Plant accessible water storage capacity and tree-scale root interactions determine how forest density reductions alter forest water use and productivity. *Frontiers in Forests and Global Change*, *2*, 36. https://doi.org/10.3389/ffgc.2019.00036

Tai, X., Anderegg, W. R. L., Blanken, P. D., Burns, S. P., Christensen, L., & Brooks, P. D. (2020). Hillslope hydrology influences the spatial and temporal patterns of remotely sensed ecosystem productivity. *Water Resources Research*, *56*(11), e2020WR027630. https://doi.org/10.1029/2020WR027630

Tai, X., Mackay, D. S., Anderegg, W. R. L., Sperry, J. S., & Brooks, P. D. (2017). Plant hydraulics improves and topography mediates prediction of aspen mortality in southwestern USA. *New Phytologist*, *213*(1), 113–127. https://doi.org/10.1111/nph.14098

Tai, X., Mackay, D. S., Sperry, J. S., Brooks, P., Anderegg, W. R. L., Flanagan, L. B., et al. (2018). Distributed plant hydraulic and hydrological modeling to understand the susceptibility of riparian woodland trees to drought-induced mortality. *Water Resources Research*, *54*(7), 4901–4915. https://doi.org/10.1029/2018WR022801

Tai, X., Venturas, M. D., Mackay, D. S., Brooks, P. D., & Flanagan, L. B. (2021). Lateral subsurface flow modulates forest mortality risk to future climate and elevated CO_2. *Environmental Research Letters*, *16*(8), 084015. https://doi.org/10.1088/1748-9326/ac1135

Thompson, S. E., Harman, C. J., Troch, P. A., Brooks, P. D., & Sivapalan, M. (2011). Spatial scale dependence of ecohydrologically mediated water balance partitioning: A synthesis framework for catchment ecohydrology. *Water Resources Research*, *47*(10). https://doi.org/10.1029/2010WR009998

Tromp-van Meerveld, H. J., & McDonnell, J. J. (2006). On the interrelations between topography, soil depth, soil moisture, transpiration rates and species distribution at the hillslope scale. *Advances in Water Resources*, *29*(2), 293–310. https://doi.org/10.1016/j.advwatres.2005.02.016

Van Mantgem, P. J., & Stephenson, N. L. (2007). Apparent climatically induced increase of tree mortality rates in a temperate forest. *Ecology Letters*, *10*(10), 909–916. https://doi.org/10.1111/j.1461-0248.2007.01080.x

Weintraub, S. R., Brooks, P. D., & Bowen, G. J. (2017). Interactive effects of vegetation type and topographic position on nitrogen availability and loss in a temperate montane ecosystem. *Ecosystems*, *20*(6), 1073–1088. https://doi.org/10.1007/s10021-016-0094-8

White, M. A., Thornton, P. E., Running, S. W., & Nemani, R. R. (2000). Parameterization and sensitivity analysis of the BIOME–BGC terrestrial ecosystem model: Net primary production controls. *Earth Interactions*, *4*(3), 1–85. https://doi.org/10.1175/1087-3562(2000)004<0003:PASAOT>2.0.CO;2

Williams, C. J., McNamara, J. P., & Chandler, D. G. (2009). Controls on the temporal and spatial variability of soil moisture in a mountainous landscape: The signature of snow and complex terrain. *Hydrology and Earth System Sciences*, *13*(7), 1325–1336. https://doi.org/10.5194/hess-13-1325-2009

Yang, Y., Donohue, R. J., & McVicar, T. R. (2016). Global estimation of effective plant rooting depth: Implications for hydrological modeling. *Water Resources Research*, *52*(10), 8260–8276. https://doi.org/10.1002/2016WR019392

Young, D. J. N., Stevens, J. T., Earles, J. M., Moore, J., Ellis, A., Jirka, A. L., & Latimer, A. M. (2017). Long-term climate and competition explain forest mortality patterns under extreme drought. *Ecology Letters*, *20*(1), 78–86. https://doi.org/10.1111/ele.12711

References From the Supporting Information

Arora, V. K., & Boer, G. J. (2003). A Representation of variable root distribution in dynamic vegetation models. *Earth Interactions*, *7*(6), 1–19. https://doi.org/10.1175/1087-3562(2003)007<0001:AROVRD>2.0.CO;2

Atkin, O. K., Bruhn, D., Hurry, V. M., & Tjoelker, M. G. (2005). Evans review No. 2: The hot and the cold: Unravelling the variable response of plant respiration to temperature. *Functional Plant Biology*, *32*(2), 87–105. https://doi.org/10.1071/FP03176

Breitmeyer, R. J., & Fissel, L. (2017). Uncertainty of soil water characteristic curve measurements using an automated evaporation technique. *Vadose Zone Journal*, *16*(13), 1–11. https://doi.org/10.2136/vzj2017.07.0136

Dingman, S. L. (2015). *Physical hydrology* (3rd ed.). Waveland Press.

Huning, L. S., & Margulis, S. A. (2018). Investigating the variability of high-elevation seasonal orographic snowfall enhancement and its drivers across Sierra Nevada, California. *Journal of Hydrometeorology*, *19*(1), 47–67. https://doi.org/10.1175/JHM-D-16-0254.1

Landsberg, J. J., & Waring, R. H. (1997). A generalised model of forest productivity using simplified concepts of radiation-use efficiency, carbon balance and partitioning. *Forest Ecology and Management*, *95*(3), 209–228. https://doi.org/10.1016/S0378-1127(97)00026-1

Xu, Q., Man, A., Fredrickson, M., Hou, Z., Pitkänen, J., Wing, B., et al. (2018). Quantification of uncertainty in aboveground biomass estimates derived from small-footprint airborne LiDAR. *Remote Sensing of Environment*, *216*, 514–528. https://doi.org/10.1016/j.rse.2018.07.022